

Article

Equity Price Dynamics under Shocks: In Distress or Short Squeeze

Cho-Hoi Hui ^{1,*}, Chi-Fai Lo ² and Chi-Hei Liu ²

¹ Banking Policy Department, Hong Kong Monetary Authority, 55/F, Two International Finance Centre, 8 Finance Street, Central, Hong Kong, China

² Institute of Theoretical Physics and Department of Physics, The Chinese University of Hong Kong, Shatin, N.T., Hong Kong, China; cflo@phy.cuhk.edu.hk (C.-F.L.); chrislch@link.cuhk.edu.hk (C.-H.L.)

* Correspondence: chhui@hkma.gov.hk; Tel.: +852-2878-1457; Fax: +852-2878-1886

Abstract: This paper proposes a simple bounded stochastic motion to model equity price dynamics under shocks. The stochastic process has a quasi-bounded boundary which can be breached if the probability leakage condition is met. The quasi-boundedness of the process at the boundary can thus provide an indicator of the possible risk of equities under price shocks or in distress. Empirical calibration of the model parameters of the proposed process for equities can be performed easily due to the availability of an analytically tractable probability density function which generates fat-tailed distributions consistent with empirical observations. The volatility and mean-reversion of the S&P500 dynamics calibrated by the process are positively and negatively co-integrated, respectively, with the VIX index representing the level of market distress. The process captures the high likelihood of Hertz's default about two months earlier, using only information until that point, and before the firm filed for Chapter 11 bankruptcy in May 2020 as a result of the COVID-19 pandemic. Empirical calibration of the process for GameStop's stock price shows that the short squeeze in the stock occurred when the condition for breaching the upper boundary was met on 14 January 2021, i.e., about two weeks before major short-sellers closed out their positions with significant losses. The trading volume of the stock was positively co-integrated with the probability leakage ratio.

Keywords: financial risk; market distress; predatory trading; short squeeze; constrained stochastic motion; quasi-bounded process; COVID-19



Citation: Hui, Cho-Hoi, Chi-Fai Lo, and Chi-Hei Liu. 2024. Equity Price Dynamics under Shocks: In Distress or Short Squeeze. *Risks* 12: 1. <https://doi.org/10.3390/risks12010001>

Academic Editors: Tak Kuen Ken Siu and Hailiang Yang

Received: 7 November 2023

Revised: 6 December 2023

Accepted: 14 December 2023

Published: 20 December 2023



Copyright: © 2023 by the authors. Licensee MDPI, Basel, Switzerland. This article is an open access article distributed under the terms and conditions of the Creative Commons Attribution (CC BY) license (<https://creativecommons.org/licenses/by/4.0/>).

1. Introduction

Black (1986) argues that an efficient market is one in which price is in the range of a factor of 2, i.e., the price is more than half of the value and less than twice the value as a result of uninformed supply and demand flows. He further argues that the factor of 2 is arbitrary, but reasonable, in light of sources of uncertainty about value and the strength of the forces tending to cause prices to return to value. Therefore, prices are within an uncertainty band in which their dynamics are not random, but exhibit trends (see de Bondt and Thaler 1985; DeLong et al. 1990; Daniel et al. 1998; Hong and Stein 1999; Asness et al. 2013; Lempérière et al. 2014; Bouchaud et al. 2019). When prices move towards the boundaries of the band, mean-reversion forces drive prices back to more mean levels. Studies including Fama and French (1988), Day and Huang (1990), Lux and Marchesi (2000), Madan (2017), and Bouchaud et al. (2018) find empirical evidence that in the dynamics of various asset classes, such as stock indexes, commodities, and currencies, mean-reversion represents a self-correcting mechanism. Nartea et al. (2021) investigate the stationarity of the daily stock prices in 12 Asia-Pacific markets during 1991–2020, and find that the stock prices became more mean-reverting and had a faster speed of adjustment towards the mean level after the global financial crisis for all sample markets. For the purposes of pricing derivatives and simulations of future prices, each stochastic process of a given

asset class has to be properly modelled to resemble its empirical statistical properties. In view of studies of the existence of uncertainty bands, price trends, and mean-reverting forces, a bounded stochastic process is needed to model the constrained stochastic motion of financial asset prices.

In this paper, we propose a relatively simple stochastic model for equity prices which are subject to either positive or negative shocks. The prices are constrained to lie between two positive bounds representing an uncertainty band. Generally, these two bounds are time-varying. Driven by forecasting with time series decomposition of equity prices, we detrend the time series of the equity prices, and the model simply concentrates on their fluctuations. The lower boundary in the proposed stochastic process is quasi-bounded, implying that the lower boundary can be breached if the probability leakage condition is met. Such a property is studied by [Pesz \(2002\)](#), [Silva et al. \(2006\)](#), and [Cardeal et al. \(2007\)](#). Similarly, completely bounded exchange rate dynamics is studied by [Ingersoll \(1997\)](#) and [Larsen and Sørensen \(2007\)](#).

Given that the well-known Cox–Ingersoll–Ross (CIR) ([Cox et al. 1985](#)) process allows the underlying variable to be quasi-bounded at the zero bound and is a mean-reverting process, we select CIR to represent the quasi-bounded process. The CIR model is popular among practitioners and is used for pricing various asset classes, such as equities, fixed income, commodities, foreign exchanges, and their derivatives, as in [Carr et al. \(2020\)](#), and modelling the variance of asset prices, as in [Heston \(1993\)](#). [Lo et al. \(2015\)](#) and [Hui et al. \(2016\)](#) find that the quasi-bounded CIR process is able to describe the exchange rate dynamics in a target zone of the HKD against the USD, and the CHF against the EUR, during September 2011 to January 2015, respectively. [Hui et al. \(2022\)](#) apply the quasi-bounded target-zone model to model yield curve control for Japanese government bonds.

The calibration of model parameters for equity prices can be performed easily, given that an analytically tractable probability density function can be derived from the CIR process. In terms of the calibrated model parameters, assessing the likelihood of future movements of equity prices becomes feasible, in particular, the likelihood of whether or not the stochastic process is still bounded. The quasi-boundedness of the process at the lower boundary can therefore provide an indicator of a possible downside risk of the corresponding equities in distress. Understanding the behaviour of distress equities has proved something of a challenge. The empirical literature documenting the distress anomaly is quite extensive, for example, [Elkamhi et al. \(2012\)](#), [Hackbarth et al. \(2015\)](#), [Gao et al. \(2017\)](#), and [Boualam et al. \(2020\)](#). Several credit risk-based theories have been developed in response to this evidence, including [Conrad et al. \(2014\)](#), [Eisdorfer et al. \(2019\)](#), [McQuade \(2018\)](#), and [Opp \(2021\)](#). The proposed quasi-bounded-process approach to studying distress equity price dynamics is different from the credit risk-based approach.

We examine whether the dynamics of the S&P500 Index (S&P) subject to market distress risk can be characterised by the quasi-bounded process. In addition, given that Hertz filed for bankruptcy (Chapter 11) due to the impact of the COVID-19 pandemic on the car-rental industry, we investigate the relationship between the intensity of the pandemic's spread, which triggered the firm's financial distress, and its equity price dynamics derived from the model. The Chapter 11 bankruptcy allowed Hertz to stay in business and restructure its obligations. Hertz was under a reorganisation plan in the best interest of the creditors. The corresponding model parameters are related to the level of market distress in terms of the VIX index and the number of COVID-19 cases, respectively, showing the validity of the model. The VIX index is a measure of constant, 30-day expected volatility derived from real-time, mid-quote prices of S&P500 Index call and put options. It is one of the most recognised measures of volatility and also captures the information of market stress conditions embedded in option prices.

Retail trading activity in the US stock market has surged since late 2019, when some brokerages cut commissions to almost zero. Its impact on the market is demonstrated by the price action of GameStop (GME) as a result of co-ordinated buying through forums in January 2021, which put the low-profile GME on the front pages of financial news

organisations. Interest in GME emerged from individual investors on social media sites after they discovered the extreme short interest in the stock (139% of free float at the peak). These investors acted as a group to build buying pressure on a short squeeze, leading GME stocks to rise 57% to USD 31.4 on 13 January 2021, followed by another 27% jump the next day. On 27 January, the share price surged to USD 347, with a median target price among analysts of only USD 12.50. On the same day, some of the most prolific hedge funds lost the majority of their GME short positions at a substantial loss (see <https://www.wsj.com/articles/melvin-capital-lost-53-in-january-hurt-by-gamestop-and-other-bets-11612103117> (accessed on 31 January 2021) and the timeline at <https://www.reuters.com/article/us-gamestop-hot-timeline-idUSKBN29W237> (accessed on 28 January 2021)).

Traders have a limited capacity, meaning that they cannot sustain losses beyond a certain point, as illustrated by Brunnermeier and Pedersen (2005), particularly for funds which have redemption obligations for investors. In addition, their trading limits, measured through value-at-risk, act as constraints on keeping their positions. When stock prices shorted (longed) by traders surge (fall) beyond certain thresholds, the positions must be closed out due to those constraints. Leverage constraints imposed by short-term creditors can also force a financial institution to liquidate long-term investments at fire-sale prices. Brunnermeier and Oehmke (2014) argue that such financial institutions may be vulnerable to predatory short-selling. Brunnermeier et al. (2009) show that the illiquidity in the market suggests more scope for predators to make a profit as those traders need more time to close out their positions with larger movements in the prices. Stein (2009) demonstrates that another destabilising impact is crowding. Boehmer et al. (2008) and Diether et al. (2009) point out that a high short-sale volume of a stock will attract positive-feedback on short-sale trading.

The mean-reversion in the CIR process represents the market actions between long-buyers and short-sellers, which form an error-correction process in the price dynamics. The process allows the equity price to be quasi-bounded at an upper bound, which is the threshold imposed by constraints such as stop-loss limits forcing traders to close out short positions squeezed by co-ordinated buying. Their scramble to buy adds to the upward pressure on the stock's price. A surge in the equity price breaching the bound triggered by the short squeeze is conditional on the probability leakage ratio of the CIR process.

This paper is organised as follows. We present the model of the quasi-bounded process in the following Section. The calibrations of the equity price dynamics under market distress and short squeezes, respectively, are presented in Section 3. The relationships between the equity dynamics and market conditions are studied empirically and discussed in Section 4. The Section 5 concludes the paper.

2. Equity Price Dynamics

2.1. Modelling Constrained Stochastic Motion

A financial observable (e.g., stock) S is constrained to move within a band $[S_L, S_U]$ for $0 \leq S_L < S_U$. Both S_L and S_U are time-varying. The moving average \bar{S} provides a trend component of the time series of S , as shown in Ritschel et al. (2021) and Vinod et al. (2022). The time series of $S - \bar{S}$ is the detrended series assuming the additive decomposition of a time series. Based on qualifying the lower boundary of the financial observable in distress, historical data of the financial observable can be used to set a trading band from which the financial observable is not expected to breach. The historical trend of the financial observable is measured based on the \bar{S} of its current and past values. For a financial observable in distress, the moving average can be scaled by a non-negative parameter, $0 < \eta_L < 1$, such that $S_L \equiv \eta_L \bar{S}$ forms a lower boundary for the movement of the financial observable. The parameter η_L , which determines the fraction of \bar{S} , suggests how much market participants expect the maximum downside of holding the financial observable. A smaller η_L indicates that the market expects wider ranges of fluctuations over a given time

horizon. Such specification of a lower boundary captures the behaviour of the financial observable over a period of time, instead of its current value.

The lower boundary S_L is defined as the number (Δ) of standard deviations (Σ) from its mean \bar{S} : $S_L = \bar{S} - \Delta\Sigma$. If a financial observable is assumed to be normally distributed and Δ is set equal to 1.5 and 2, respectively, suggesting that falling to the lower boundary means it is in distress, the corresponding cumulative normal probabilities of the financial observable falling below the boundaries are 0.0668 and 0.0227. This approach was used in a study of currency crashes by Jurek (2014), in which the crash level was set at 0.7 and 1.4 standard deviations, respectively, away from the spot exchange rates. This measure is also similar to value-at-risk (VaR), which is defined as the maximum expected loss of assets or portfolios at a pre-defined confidence level (say 95%) over a given time horizon. In other words, a 5% probability of such extreme loss suggests that the asset price is under stress. As long as the level of the boundary is adequately low, the choice of its level does not affect the process of the financial observable dynamics.

The upper boundary can be defined similarly as $S_U \equiv \eta_U \bar{S}$ for a parameter $\eta_U > 1$. The logarithm normalised fractional deviation x of S from \bar{S} is given by

$$x = -\ln \left[\frac{\eta_U \bar{S} - S}{(\eta_U - \eta_L) \bar{S}} \right], \quad (1)$$

where $x \in [0, \infty]$, and $x = 0$, when $S = S_L$. Both η_U and η_L are adjustable parameters for the upper and lower boundaries of a band, respectively. It is not necessary for the two time-varying boundaries to be symmetric about the moving average \bar{S} . Accordingly, it is clear that the financial observable is confined to a drifting band with time-varying width. Similarly, regarding an upside shock, we can put the origin $x' = 0$ at an upper boundary by defining

$$x' = -\ln \left[\frac{S - \eta_L \bar{S}}{(\eta_U - \eta_L) \bar{S}} \right]. \quad (2)$$

The stochastic process of a financial asset is commonly modelled by the CIR process (see, for example, Heston 1993). The CIR process allows the underlying variable to be quasi-bounded at the zero bound and is a mean-reverting process. Following this approach, we propose that the normalised financial observable x in Equation (1) (x' in Equation (2)) follows the CIR process:

$$dx = \kappa(\theta - x)dt + \sigma_x \sqrt{x}dZ, \quad (3)$$

where dZ is a Wiener process with $E[dZ] = 0$ and $E[dZ^2] = dt$. Here, $\sigma_x \sqrt{x}$ in the second stochastic term depends on the level of x , and κ determines the speed of the mean-reverting drift towards the long-term mean θ . According to Feller's classification of boundary points, the one at the origin is a boundary of no probability leakage under the condition $(\sigma_x^2 / 4\kappa\theta) < 1$ (see Karlin and Taylor 1981). In other words, it is a quasi-bounded process, and x could breach the boundary if the no-leakage condition is not met. The infinity is a non-attractive natural (or inaccessible) boundary.

The normalised financial observable x , which is a fractional deviation of S from \bar{S} , follows the CIR process by using the normalisation of Equation (1) or (2). The implication is that the normalised financial observable dynamics contain information on the random fluctuation of S . A mean-reverting force in the financial observable dynamics will pull the random variable x away from the lower (upper) boundary towards the mean level. Probability leakage through the quasi-bounded boundary occurs only in rare situations when fluctuations accompanied by a shock in the financial observable surge drastically or the mean-reverting force diminishes sharply. This condition is consistent with the observations in Bates (2012), in which volatility goes up or an error-correction process drops during economic recessions.

2.2. Probability Density Function

The probability density function (PDF) of x under the CIR process is given by:

$$G(x, t; x', t') = \frac{2}{\sigma_x^2 C_1(t-t')} \left(\frac{x}{x'}\right)^{\omega/2} \exp\left[-\frac{\omega+2}{2} C_2(t-t')\right] \times \exp\left\{-\frac{2x'+2x \exp[-C_2(t-t')]}{\sigma_x^2 C_1(t-t')}\right\} \times I_{\omega}\left\{\frac{4x^{1/2}x'^{1/2} \exp[-C_2(t-t')/2]}{\sigma_x^2 C_1(t-t')}\right\}, \tag{4}$$

where $\omega = 2\kappa\theta/\sigma_x^2 - 1$, $C_1(\tau) = [\exp(\kappa\tau) - 1]/\kappa$, and $C_2(\tau) = -\kappa\tau$, and I_{ω} is the modified Bessel function of the first kind of order ω . The associated asymptotic PDF will eventually approach the steady-state distribution, which is:

$$K(x, t \rightarrow \infty, x', t') = \frac{2x^{\omega}}{\Gamma(\omega + 1)} \left(\frac{2\kappa}{\sigma_x^2}\right)^{\omega+1} \exp\left(-\frac{2\kappa}{\sigma_x^2} x\right), \tag{5}$$

where Γ is the gamma function. Given the PDF in Equation (4), the parameters of the CIR process are calibrated by using market data in Section 3.

Based on the calibration of the model parameters using the S&P in Section 3, and setting the lower boundary at $\eta_L S_{At} = S_L = 1900$ and upper boundary at $\eta_U S_{At} = S_U = 3320$, the steady-state distributions in S with three values of the long-term mean θ of 0.3, 1.0, and 1.5 are shown in Figure 1. The smaller θ is closer to the lower boundary with $S = 2268$, 2797, and 3003, respectively. We use the model parameters for $\sigma_x = 0.05$ (Panel A), and 0.15 (Panel B), and $\kappa = 0.05$. The distributions peak at $\theta = 1.0$ and 1.5 on the right, indicating a left-fat-tails effect with the probability of outlier negative returns. However, using $\theta = 0.3$, the distributions peak on the left with a fat tail on the right. The different skewness of the distributions is consistent with both left- and right-skewed distributions obtained from empirical observations of equity returns, depending on their sample periods. We performed a comparison between Panels A and B, where σ_x increases from 0.05 to 0.15, and the distributions have fatter tails and become hump-shaped. The distributions generated from the quasi-bounded process show that the probability leakage condition is consistent with the empirical left-skewed distributions for equities in distress.

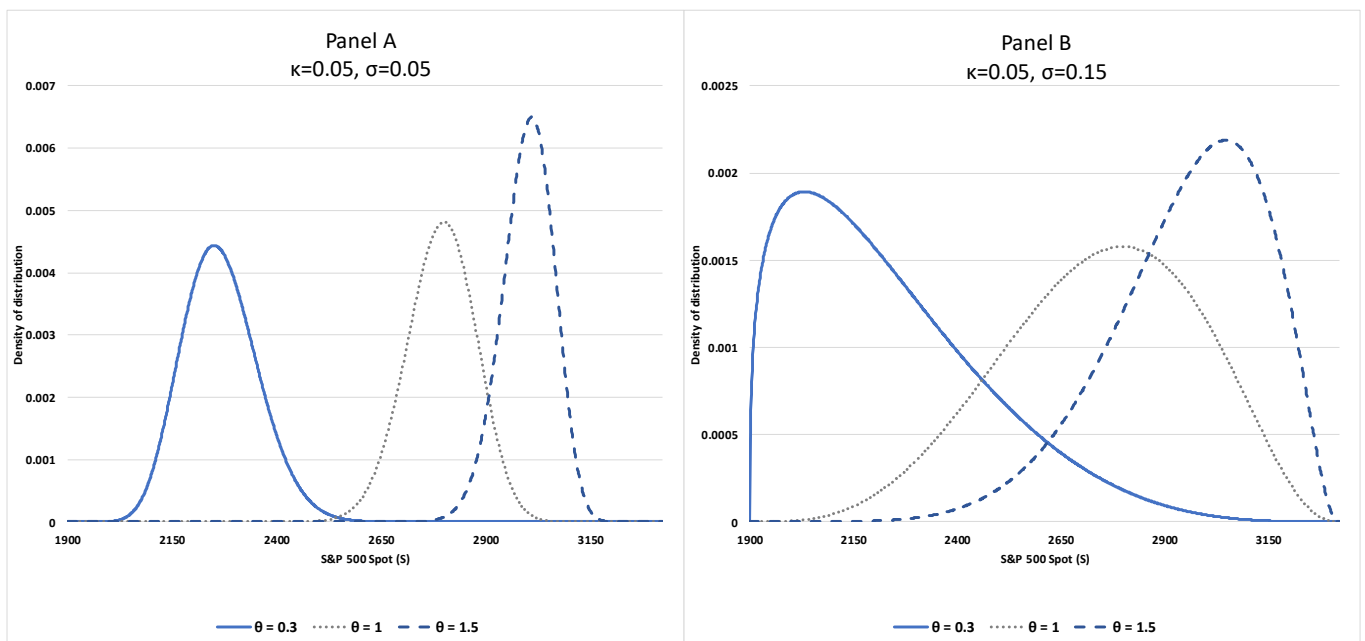


Figure 1. S&P500 Index distributions with different values of model parameters σ_x , κ , and θ under normalisation on 1 November 2018. Panel (B) illustrates the distributions with $\sigma_x = 0.15$, which is higher than $\sigma_x = 0.05$ used in Panel (A).

3. Model Calibration

3.1. Calibrations of S&P500 Index in Distress

We examine whether the dynamics of the S&P in distress can be characterised by the quasi-bounded process. The model parameters of the process specified in Equation (3) are calibrated based on the PDF of Equation (4) and the logarithm-normalised x in Equation (1). The calibration employs maximum likelihood estimation (MLE) of the time series of the daily spot index of the S&P data from 1 January 1990 to 20 June 2020. Figure 2 (Panel A) shows the S&P in S and the associated moving lower and upper boundaries with the parameters of $\eta_L = 0.7$ and $\eta_U = 1.2$ with the 50-day moving average, and the normalised index in x . The estimation is based on a 1-year rolling window. The market data used for the estimations are from Bloomberg.

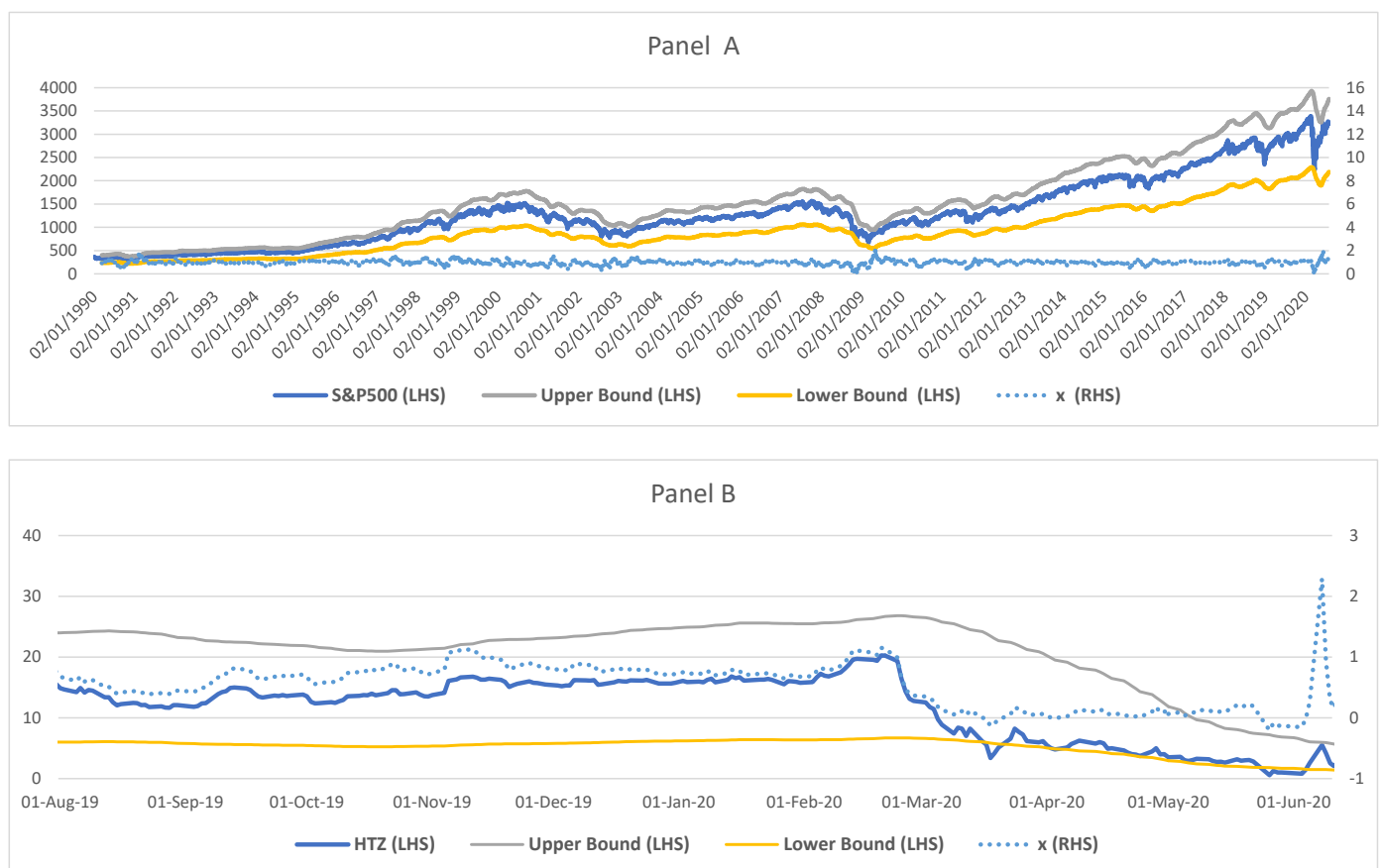


Figure 2. S&P500 Index (Panel A) and Hertz stock price (Panel B) in S -scale and x -scale, and upper and lower boundaries in S with $\eta_L = 0.7$ and $\eta_U = 1.2$ for S&P500 Index and $\eta_L = 0.25$ and $\eta_U = 1.75$ for Hertz stock price with 50-day moving average.

Figure 3 reports the estimates of drift κ (Panel A) at a 5% significance level with its z -statistic above 1.96 when κ is above 0.02. κ was in the range from 0.02 to 0.12 for most of the time and dropped sharply under shocks or crashes in the market. As the S&P dropped towards its lower boundary when the market crashed, the mean-reverting force weakened with the dropped κ . The estimation of κ became insignificant (not significantly different from zero) in very short periods of time after the crashes. Subsequently, the estimation rebounded to the 0.04 level and was significant. Panel B shows a significant steady mean θ with values ranging between 0.7 and 1.2. The estimation of θ became insignificant in very short periods of time after the crashes, similar to the changes in κ . The mean-reversion represented by κ and θ was found to be present in the estimations.

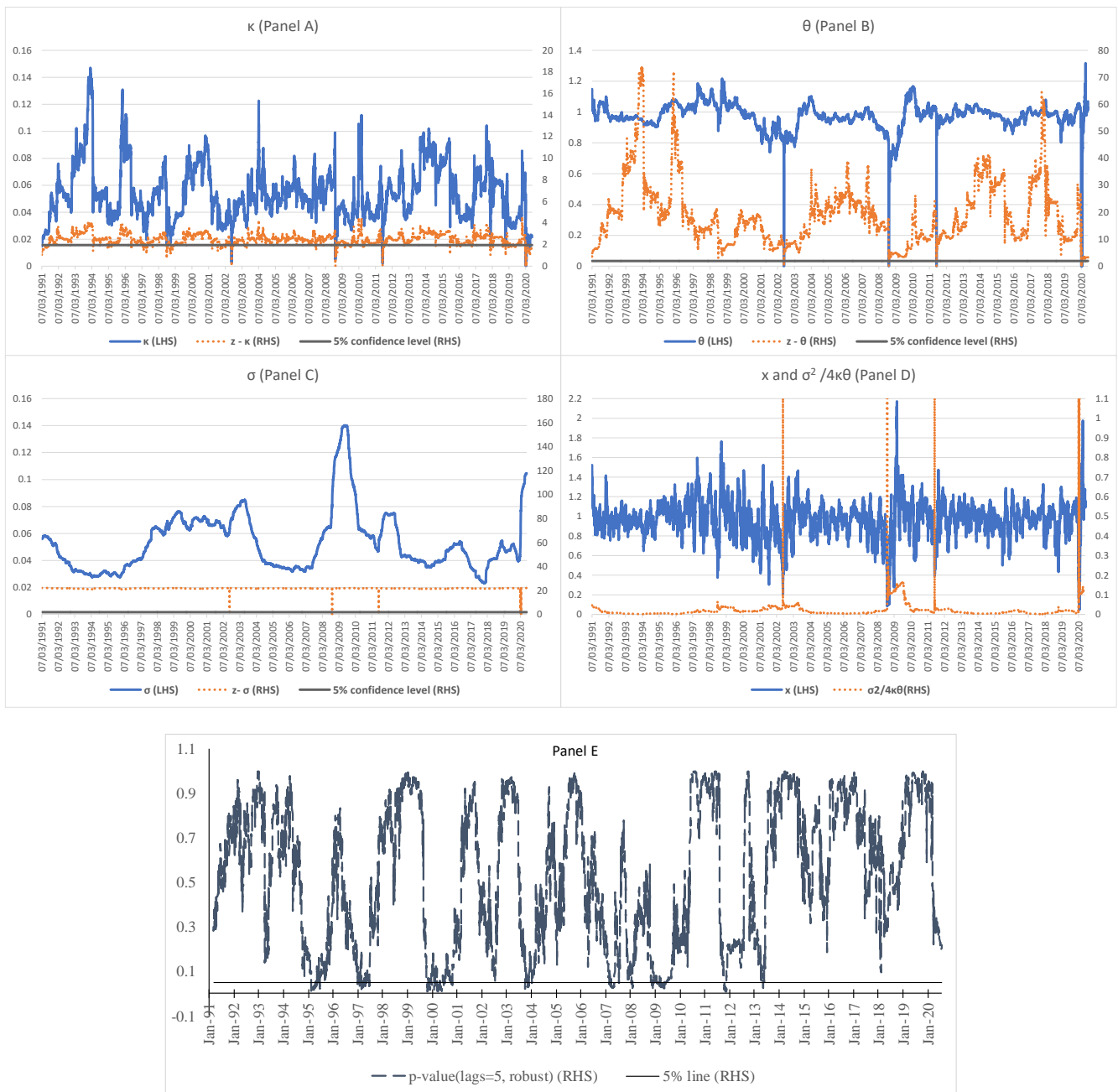


Figure 3. Estimated κ (Panel A), θ (Panel B), σ_x (Panel C), corresponding z-statistic, leakage ratio ($\sigma_x^2/4\kappa\theta_x$) (Panel D) of S&P500 Index using 1-year rolling window, and test on residuals (Panel E).

The volatility σ_x in Panel C is estimated to be significant between 0.02 and 0.14. The results suggest that the volatility part of the quasi-bounded dynamics is robust. The volatility increased sharply during 2008–2009 when the global financial crisis emerged, and during the COVID-19 outbreak in March 2020.

Panel D displays the leakage condition of ($\sigma_x^2/4\kappa\theta$) to identify periods when this measure is greater than 1 to portray the crash risk of the S&P at the lower boundary. The measure was generally below 0.01, suggesting that the crash risk was immaterial when the S&P was well bounded above the lower boundary. In recent history, the measure rose sharply and breached 1.0 on 23 July 2002 (the dotcom bubble crash), 9 October 2008 (the subprime mortgage crisis), 8 August 2009 (the global financial crisis), and 9 March 2020 (the COVID-19 pandemic), with the existence of the leakage condition. The diminishing

mean-reverting force in the S&P dynamics and the leakage condition reflect the crash risk being built up during those periods of financial distress.

We use the Breusch–Godfrey serial correlation Lagrange-multiplier test to study auto-correlation in the errors of the model estimations. The test uses the residuals from the model, and the corresponding test statistic is derived from these. The null hypothesis is that there is no serial correlation of any order up to p . Panel E shows that despite some rejections of null hypothesis (i.e., low p -values), the majority of the tests support the hypothesis that the residuals are not serially correlated up to 5 days, indicating that the estimations are adequate.

3.2. Calibrations of Hertz Equity Price in Distress

To investigate how financial distress affects equity price dynamics, we calibrate the dynamics of the Hertz equity (HTZ) price according to the quasi-bounded process. Hertz filed voluntary petitions for re-organisation under Chapter 11 on 22 May 2020 as the COVID-19 pandemic crushed the car-rental industry. The sample period covers the daily price of HTZ from 18 August 2014 to 31 August 2020. Panel B of Figure 2 shows the price of HTZ in S and the associated moving lower and upper boundaries with the parameters of $\eta_L = 0.4$ and $\eta_U = 1.6$ with the 50-day moving average, and the normalised price in x . The lower and upper boundaries correspond to about 2.4 standard deviations, respectively. The estimations are based on the 2-year rolling window.

Figure 4 reports the estimated drift term κ (Panel A) at the 5% significance level when κ is above 0.02. κ was between 0.02 and 0.1 during most of the time. It dropped sharply and was not significantly different from zero on 16 March 2020. As the HTZ price dropped towards its lower boundary during March 2020, the mean-reverting force in its dynamics weakened substantially. Panel B shows a significant steady estimated mean θ ranging between 0.5 and 0.8, which became insignificant on 16 March 2020. The volatility σ_x displayed in Panel C is estimated to be highly significant, with a value between 0.06 and 0.13.

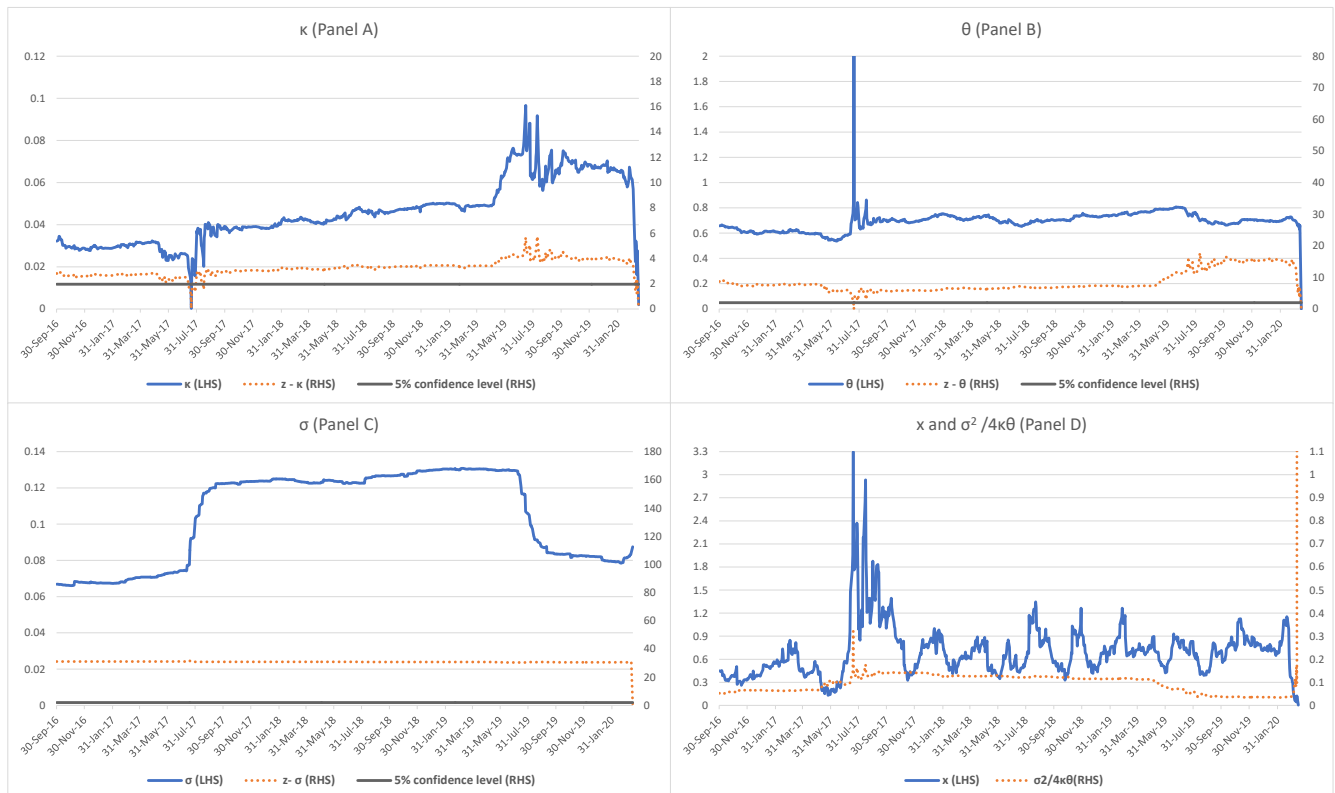


Figure 4. Estimated κ (Panel A), θ (Panel B), σ_x (Panel C), corresponding z-statistic, and leakage ratio ($\sigma_x^2/4\kappa\theta_x$) (Panel D) of Hertz stock price using 2-year rolling window.

Panel D shows the measure of the probability leakage condition, which was below 0.2 before March 2020, suggesting that the default risk was not significant as the HTZ price was bounded above the lower boundary. The measure rose sharply and breached 1.0 on 16 March 2020 with the existence of the leakage condition when the HTZ price fell sharply. While the HTZ price was bounded above the lower boundary for much of the time, as indicated by its dynamics, the condition for breaching the boundary was met on 16 March 2020 using only information until that point, about two months before the company filed for bankruptcy. The existence of the leakage condition suggests that the default risk of the firm occurs and its default probability accumulates.

3.3. Calibration of GameStop Stock Price Dynamics under Short Squeezes

The calibration was conducted by applying the MLE and the logarithm normalised in Equation (2) to the daily GME price data from 1 January 2017 to 21 January 2021. Figure 5 (Panel A) shows the GME price in S and the moving upper boundary with $\eta_U = 2.5$ with the 50-day moving average, and the equity price in x . The upper boundary is about 2.5 standard deviations, covering the probability of 99.38%.

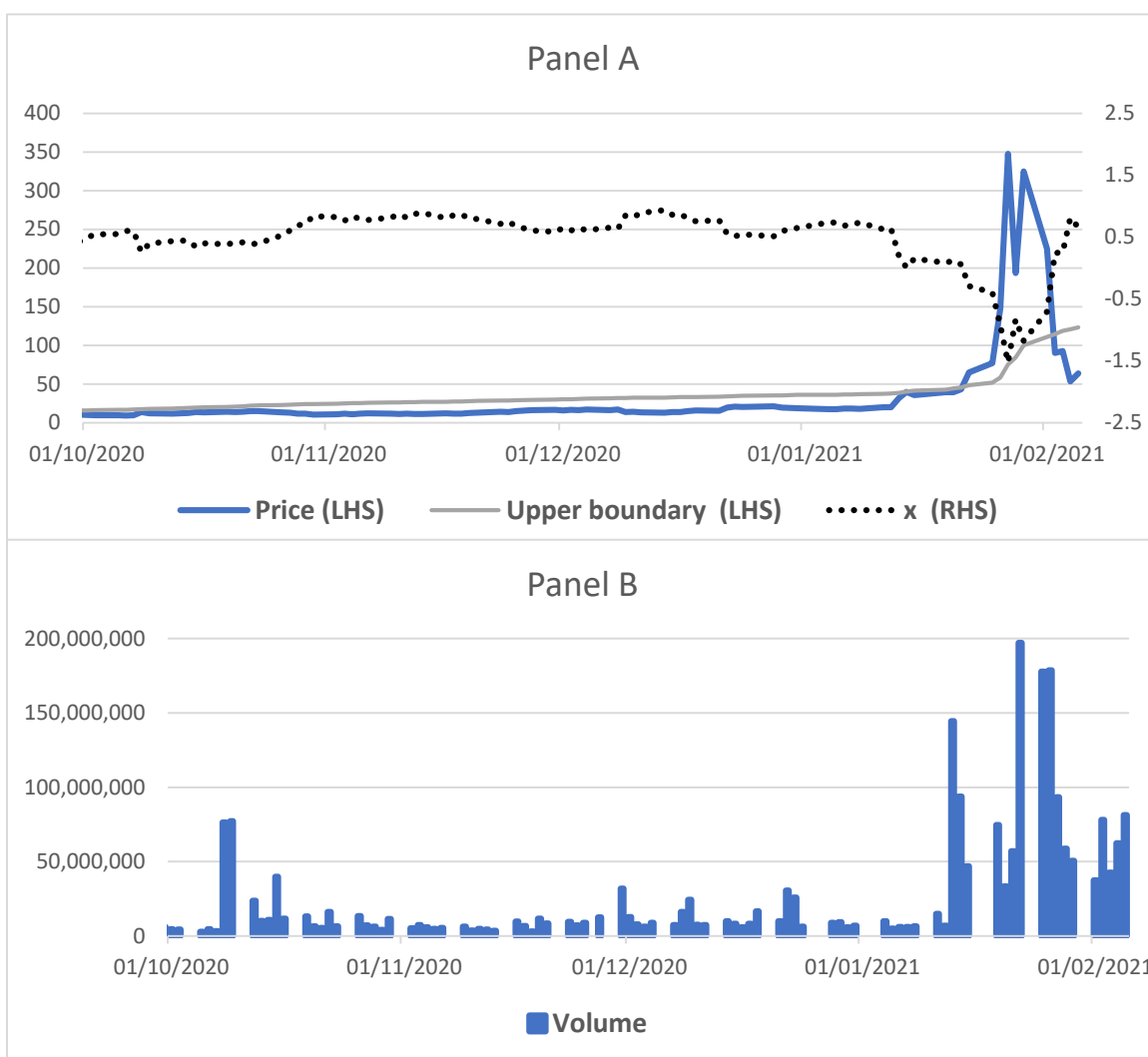


Figure 5. GameStop stock price in S -scale and x -scale and upper boundary [$\eta_U = 2.5$] in S with 50-day moving average (Panel A) and trading volume (Panel B).

Using the 2-year rolling window, Figure 6 reports the estimates of the drift term κ (Panel A), which are statistically significant at the 5% significance level. When the GME

price surged sharply in January 2021, κ fell and was not significantly different from zero on 14 January 2021. Panel B shows the estimated mean θ , which is significant, with the corresponding z-statistic above the 1.96 level until the price spiked in January 2021. The results show that the mean-reverting force in terms of κ and θ was present in the GME price dynamics during the estimation period and diminished under the short squeeze in January 2021. The volatility σ_x of the quasi-bounded process, which is displayed in Panel C, is estimated to be highly significant and to have an increasing trend with a jump in January 2021.

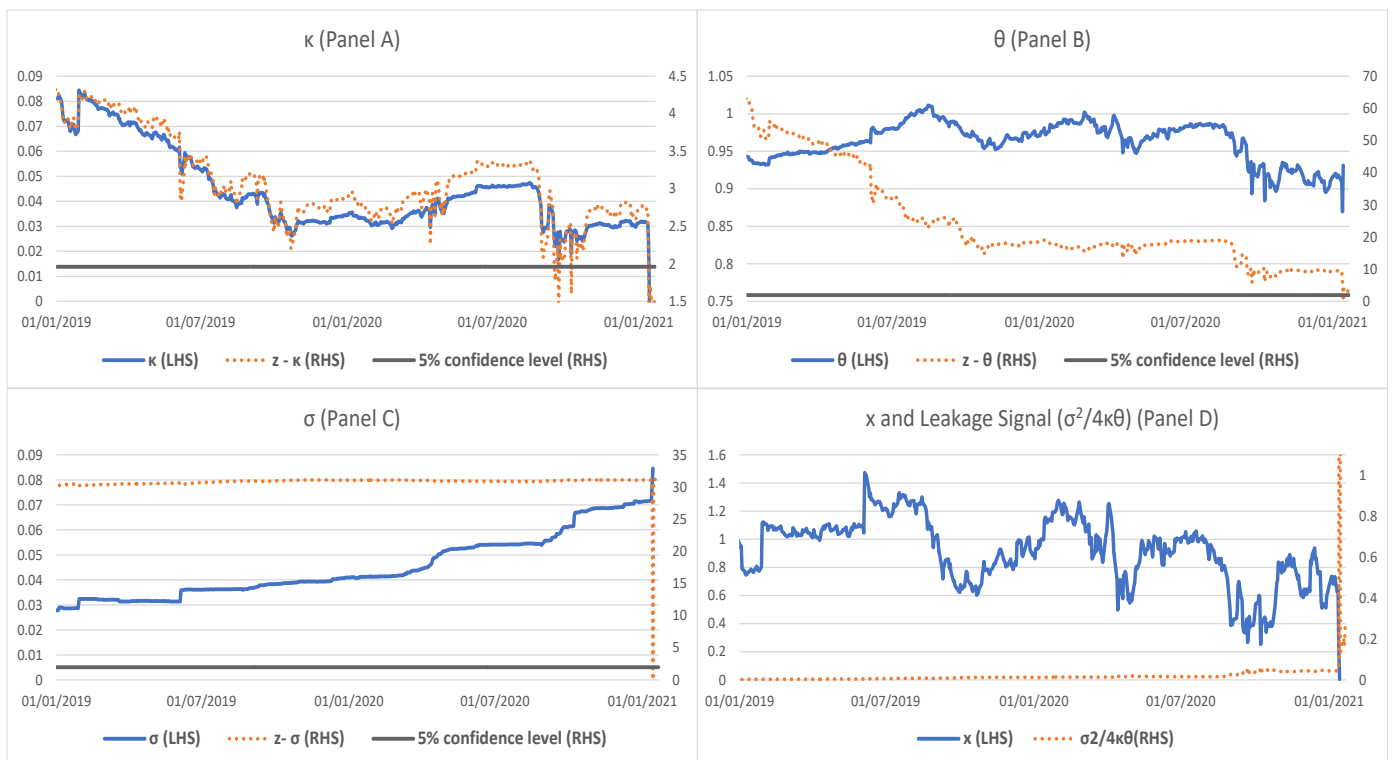


Figure 6. Estimated κ (Panel A), θ (Panel B), σ_x (Panel C), corresponding z-statistic, and leakage ratio ($\sigma_x^2/4\kappa\theta_x$) (Panel D) of GameStop stock price with 50-day moving average using 2-year rolling window.

As the probability leakage condition of $(\sigma_x^2/4\kappa\theta)$ portrays the likelihood of the GME price breaching the upper boundary under the short squeeze, Panel D displays this measure to identify when the leakage condition is greater than 1. The measure was, in general, below 0.05, suggesting that the short squeeze was not relevant to the GME price bounded below the upper boundary. The measure rose sharply and breached 1.0 on 14 January 2021 with a leakage condition greater than 1 when the GME price escalated. The diminishing mean-reverting force in the GME price dynamics and the existence of the leakage condition indicate that the short squeeze built up through co-ordinated buying.

4. Discussion

4.1. The Dynamic Relationship of S&P500 Index Dynamics with Market Stress Condition

To test the validity of incorporating crash/distress risk into the model, a co-integration analysis is used in this paper to test the relationship between the dynamics of the S&P and the VIX. The VIX measures the level of risk aversion anticipated by market participants to put capital into the market. This is noted as the model parameters based on the MLE are estimated using the S&P data only, without any information from the option market.

We use the following dynamical error-correction representation to investigate any long-run equilibrium relationship between the model parameters and VIX:

$$\Delta y_t = a_{10} + \alpha_y(y_{t-1} - \beta_1 X_{t-1}) + \sum_k b_{1k} \Delta y_{t-k} + \sum_k c_{1k} \Delta X_{t-k} + \varepsilon_{yt}, \quad (6)$$

where y_t is either κ , S_θ , or σ_x at time t ; α_y is negative; and X_{t-1} is the logarithm of the VIX at time $t - 1$. y_t represents the logarithm of model parameters (κ , σ_x), and the mean level S_θ will respond to stochastic shocks represented by ε_{yt} and the long-run equilibrium deviation in the previous period ($y_{t-1} - \beta_1 X_{t-1}$). The mean level S_θ in the original price measure of S is used instead of θ , because risk sentiment in the market is based on the level of the price in S , not in x normalised by the time-varying upper and lower boundaries. The co-integration relationship specification of error-correction requires that the estimated speed of adjustment (i.e., α_y) should be negative and nonzero. A larger α_y in absolute terms indicates higher sensitivity of y_t to the long-run equilibrium deviation.

As there was a structural break during the global financial crisis in 2009, the estimation is conducted at a daily frequency for the pre-crisis period from 1 January 2001 to 31 December 2009, and the post-crisis period from 1 January 2011 to 30 June 2020. The summary statistics, correlation coefficient, and respective Augmented Dickey–Fuller (ADF) test results for the variables, both in the levels and the first differences, for the pre- and post-crisis periods, respectively, are reported in Table 1. The ADF test results show that $\ln(\kappa)$, $\ln(S_\theta)$, $\ln(\sigma_x)$, and the logarithm value of the VIX [$\ln(VIX)$] have a unit root in level. However, these variables are co-integrated with the same order $I(1)$ given the lack of presence of a unit root at the 1% level for their first differences.

We adopt the single-equation test in [Engle and Granger \(1987\)](#) to test the co-integration relationship between [$\ln(\kappa)$, $\ln(S_\theta)$, $\ln(\sigma_x)$] and $\ln(VIX)$. It tests the stationarity of the residuals of the linear combinations between i. $\ln(\kappa)$ and $\ln(VIX)$; ii. $\ln(S_\theta)$ and $\ln(VIX)$; and iii. $\ln(\sigma_x)$ and $\ln(VIX)$. The co-integration tests between $\ln(VIX)$ and [$\ln(\kappa)$, $\ln(S_\theta)$, $\ln(\sigma_x)$] are reported in Table 2 for the pre- and post-crisis periods, respectively. On the whole, the results show that there is at least one co-integrating vector of $\ln(VIX)$ and [$\ln(\kappa)$, $\ln(S_\theta)$, $\ln(\sigma_x)$], respectively, given the statistical significance at the 1% or 5% level.

Table 3 shows that the co-integrating vectors expressed by β between $\ln(VIX)$ and [$\ln(\kappa)$, $\ln(S_\theta)$, $\ln(\sigma_x)$] are estimated to be $[-0.2, -0.14, 0.83]$ and $[-0.52, -0.14, 0.56]$ in the pre-crisis and post-crisis periods, respectively, at the 1% significance level. The estimated negative coefficients indicate that a higher VIX would decrease κ and S_θ . The negative relationship suggests that when the VIX increases, the crash risk of the S&P rises, with a weakened mean-reverting force in the S&P dynamics. On the other hand, the estimated positive coefficient for σ_x shows that a higher VIX would increase σ_x as expected.

Table 4 reports the estimates of the speed of adjustment (α_y) for [$\ln(\kappa)$, $\ln(S_\theta)$ and $\ln(\sigma_x)$], which are negative, with $[-0.04, -0.005, -0.04]$ and $[-0.01, -0.001, -0.0045]$, in the pre-crisis and post-crisis periods, respectively, suggesting that the model parameters will adjust to recover the long-run equilibrium. The error-correction specification is thus valid, with the presence of a self-restoring force, such that the gaps between the model parameters and VIX will be closed.

Table 1. Descriptive statistics of $\ln(\kappa)$, $\ln(S_\theta)$, and $\ln(\sigma_x)$ for S&P500 Index and $\ln(\text{VIX})$.

1 January 2001–31 December 2009												
	$\ln(\kappa)$		$\ln(S_\theta)$		$\ln(\sigma)$		$\ln(\text{vix})$					
	Level	Change	Level	Change	Level	Change	Level	Change	Level	Change		
Mean	−3.02	0.000	6.94	0.000	−2.87	0.000	3.00	−0.002				
Median	−3.01	0.000	6.96	0.000	−2.81	0.000	3.00	−0.006				
Maximum	−2.10	2.134	7.29	0.239	−1.97	0.088	4.39	0.496				
Minimum	−5.86	−2.167	6.59	−0.251	−3.45	−0.038	2.29	−0.300				
Std. Dev.	0.27	0.081	0.16	0.010	0.43	0.006	0.41	0.059				
Skewness	−1.01	−0.490	−0.23	−9.265	0.39	2.627	0.50	0.548				
Kurtosis	12.24	469.397	2.09	604.122	2.17	39.756	2.92	7.483				
ADF test statistics	0.09	−24.35	***	−1.21	−19.46	***	−0.13	−4.583	***	−1.56	−50.95	***
Phillips–Perron test statistics	0.10	−59.40	***	−1.90	−57.26	***	−0.48	−55.546	***	−2.94	−53.32	***
Correlation with $\ln(\text{vix})$	−0.303	-	−0.413	-	0.802	-	-	-	-	-	-	-
Observations	2236	2140	2262	2179	2263	2181	2263	2181				
1 January 2011–30 June 2020												
	$\ln(\kappa)$		$\ln(S_\theta)$		$\ln(\sigma)$		$\ln(\text{vix})$					
	Level	Change	Level	Change	Level	Change	Level	Change	Level	Change		
Mean	−2.94	0.000	7.48	0.000	−3.09	0.000	2.78	−0.001				
Median	−2.87	0.001	7.52	0.001	−3.12	0.000	2.71	−0.007				
Maximum	−2.26	0.372	8.27	0.297	−2.26	0.130	4.42	0.768				
Minimum	−13.82	−0.321	6.96	−0.301	−3.77	−0.080	2.21	−0.314				
Std. Dev.	0.43	0.048	0.29	0.014	0.28	0.008	0.33	0.080				
Skewness	−8.09	−0.234	−0.20	2.802	0.29	4.180	1.35	1.231				
Kurtosis	190.56	11.297	1.94	435.728	3.61	64.434	5.52	9.968				
ADF test statistics	−0.86	−49.86	***	−1.49	−49.08	***	−0.91	−13.17	***	−1.03	−50.90	***
Phillips–Perron test statistics	−0.86	−49.77	***	−2.02	−75.27	***	−0.61	−44.89	***	−0.97	−54.12	***
Correlation with $\ln(\text{vix})$	−0.357	-	−0.162	-	0.622	-	-	-	-	-	-	-
Observations	2312	2211	2386	2296	2389	2301	2389	2302				

Notes: *** indicates significance at a level of 1%. Both tests check the null hypothesis of unit root existence in the time series.

Table 2. Tests for co-integration of $\ln(\kappa)$, $\ln(S_\theta)$, and $\ln(\sigma_x)$ for S&P500 Index and $\ln(\text{VIX})$.

Engle–Granger Single-Equation Test Dependent Variable:	1 January 2001–31 December 2009					
	$\ln(\kappa)$		$\ln(S_\theta)$		$\ln(\sigma)$	
ADF test statistic	−5.01	***	−1.95	**	−3.66	***
Phillips–Perron test statistic	−7.09	***	−2.59	***	−3.62	***

Engle–Granger Single-Equation Test Dependent Variable:	1 January 2011–30 June 2020					
	$\ln(\kappa)$		$\ln(S_\theta)$		$\ln(\sigma)$	
ADF test statistic	−3.55	***	−6.46	***	−4.47	***
Phillips–Perron test statistic	−3.19	***	−4.54	***	−3.59	***

Notes: *** and ** indicate significance at levels of 1% and 5%, respectively. The co-integration test uses the Augmented Dickey–Fuller and Phillips–Perron tests to check the null hypothesis that the residuals of the regression of $\ln(\text{VIX})$ and the parameters from the MLE calibration with the 3-year rolling window are non-stationary, assuming zero mean in the test equation. The critical value of the test was obtained from [MacKinnon \(1996\)](#).

Table 3. Estimates of long-run coefficient (β) $\ln(\kappa)$, $\ln(S_\theta)$, and $\ln(\sigma_x)$ for S&P500 Index and $\ln(\text{VIX})$.

Dependent Variable:	1 January 2001–31 December 2009					
	$\ln(\kappa)$		$\ln(S_\theta)$		$\ln(\sigma)$	
$\ln(\text{vix})$	−0.20	***	−0.14	***	0.83	***
Constant	−2.41	***	7.38	***	−5.36	***

Dependent Variable:	1 January 2011–30 June 2020					
	$\ln(\kappa)$		$\ln(S_\theta)$		$\ln(\sigma)$	
$\ln(\text{vix})$	−0.52	***	−0.14	***	0.56	***
Constant	−1.51	***	7.89	***	−4.65	***

Notes: *** indicates significance at a level of 1%.

Table 4. Estimation results of the short-run dynamics for $\ln(\kappa)$, $\ln(S_\theta)$, and $\ln(\sigma_x)$ for S&P500 Index and $\ln(\text{VIX})$.

Dependent Variable:	1 January 2001–31 December 2009					
	$\ln(\kappa)$		$\ln(S_\theta)$		$\ln(\sigma)$	
$\ln(\text{vix})$						
Speed of adjustment	−0.04	***	−0.005	*	−0.04	***
Lag length	2		2		2	

Dependent Variable:	1 January 2011–30 June 2020					
	$\ln(\kappa)$		$\ln(S_\theta)$		$\ln(\sigma)$	
$\ln(\text{vix})$						
Speed of adjustment	−0.0100	***	−0.001	*	−0.0045	***
Lag length	5		26		3	

Notes: *** and * indicate significance at levels of 1% and 10%, respectively.

4.2. The Relationship between Hertz Equity Price Dynamics and COVID-19

Given that Hertz filed for Chapter 11 due to the impact of the COVID-19 pandemic on the car-rental industry, we investigate the relationship between the intensity of the pan-

demic's spread, which triggered the firm's financial distress, and its equity price dynamics derived from the model. We estimate the simple linear regression as follows:

$$\ln(y_t) = a + b\ln(\text{COVID19}), \quad (7)$$

where y_t is the model parameters $\{\kappa, \theta, \sigma_x\}$, COVID19 is the number of new confirmed COVID-19 cases in the US, and a and b are the coefficients to be estimated.

As the first confirmed COVID-19 case in the US was on 22 January 2020 and the quasi-bounded process for HTZ was no longer bounded after 16 March 2020, the estimation is conducted for the period between these two dates. Figures 7–9 show the scatter plots of the model parameters and the number of daily new COVID-19 cases in the US in logarithm. The data of COVID-19 cases were compiled by the Johns Hopkins University Center for Systems Science and Engineering (JHU CCSE) from various sources and can be found at <https://data.humdata.org/dataset/novel-coronavirus-2019-ncov-cases> (accessed on 15 September 2020). The coefficients $[a, b]$ are estimated to be $[-2.37, -0.16]$ for κ , $[-0.32, -0.01]$ for θ , and $[-2.55, 0.019]$ for σ_x , respectively. All the estimates of coefficients are statistically significant at the 1% level. The R^2 of 0.777, 0.463, and 0.737 for κ , θ , and σ_x , respectively, are reasonably high.

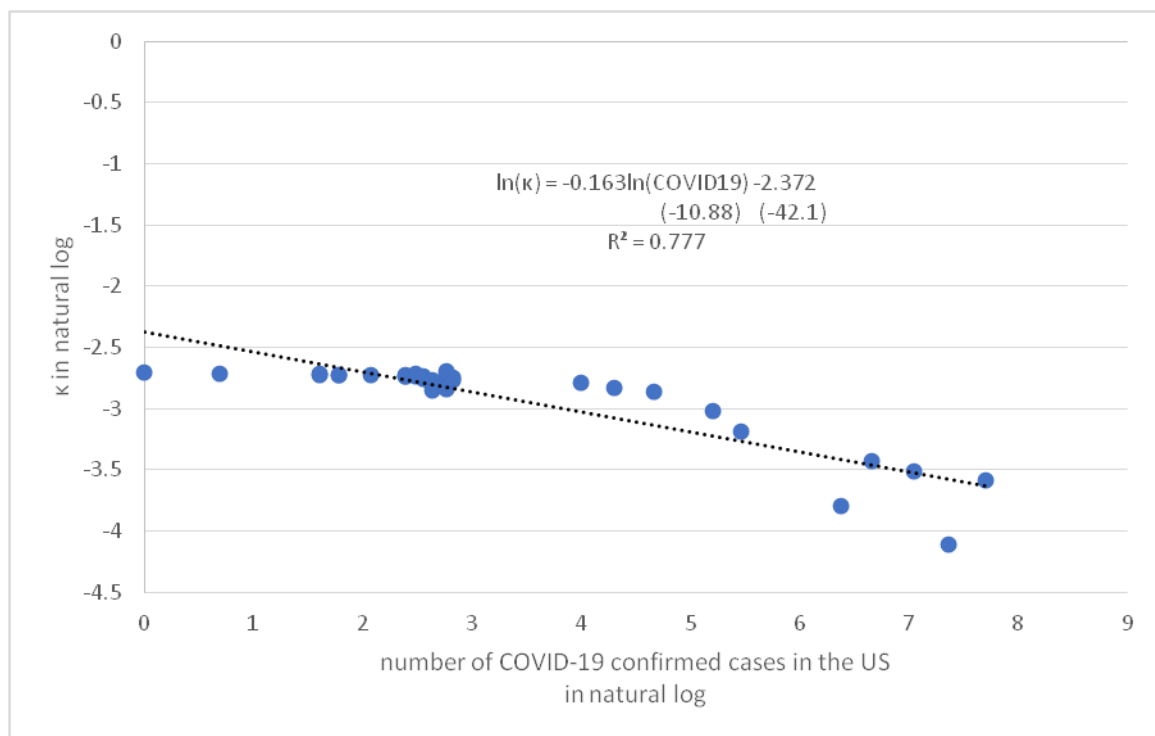


Figure 7. A simple regression of $\ln(\kappa) = a + b\ln(\text{COVID-19})$ with t -statistic in parentheses for Hertz stock price.

The negative coefficients b_κ and b_θ show a negative relationship between the mean-reversion (represented by κ and θ) and the number of COVID-19 cases in the US. Conversely, the relationship in terms of b_{σ_x} between the volatility σ_x and the number of confirmed cases is positive. An increase in the number of confirmed cases weakened the mean-reverting force, but enhanced the volatility in the HTZ price dynamics, suggesting an increased default risk for the firm due to the COVID-19 pandemic in the US. These results are consistent with those of the model calibration results and the measure of the probability leakage condition at the lower boundary for the HTZ price in Section 3.2.

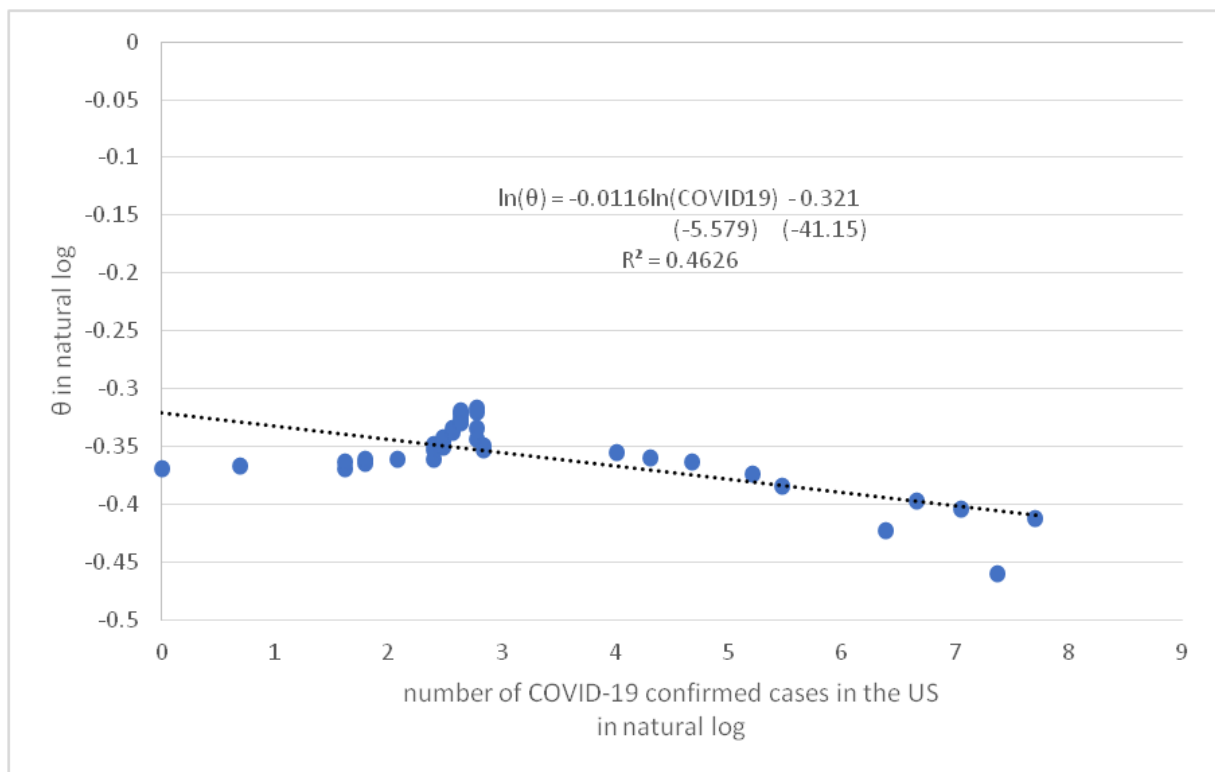


Figure 8. A simple regression of $\ln(\theta) = a + b\ln(\text{COVID-19})$ with t -statistic in parentheses for Hertz stock price.

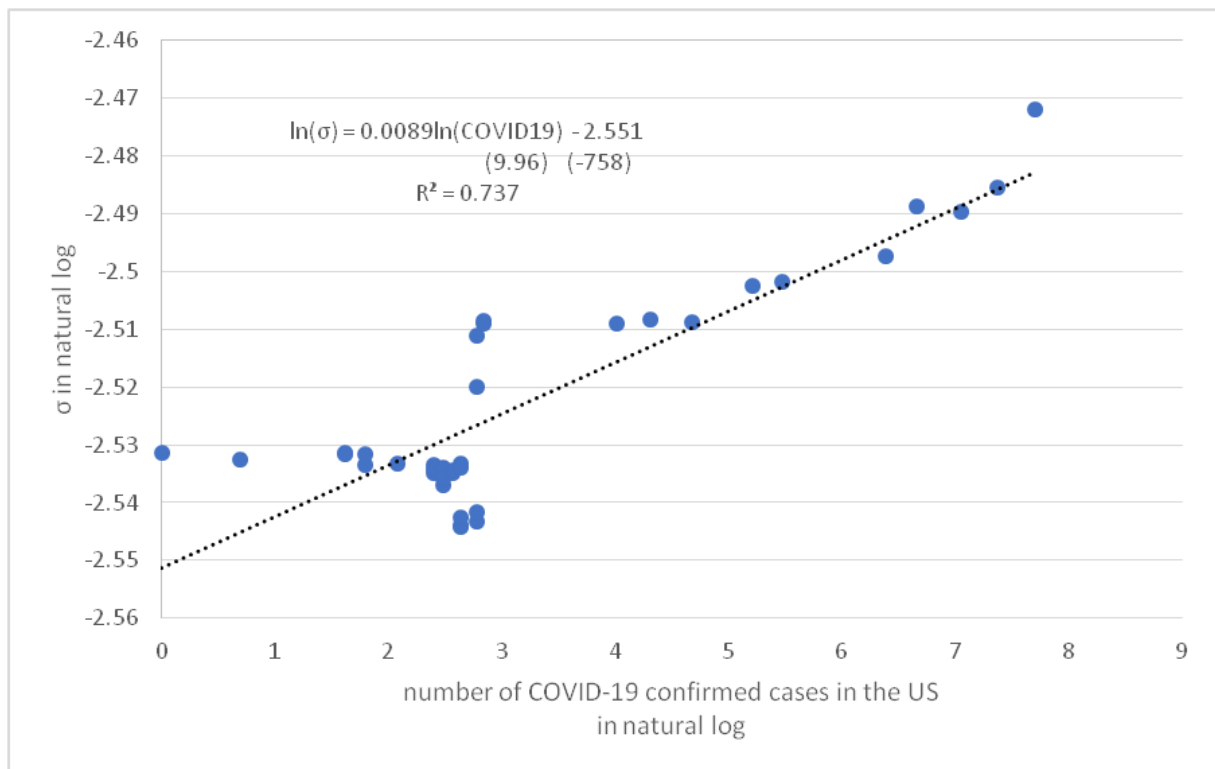


Figure 9. A simple regression of $\ln(\sigma_x) = a + b\ln(\text{COVID-19})$ with t -statistic in parentheses for Hertz stock price.

4.3. The Relationship between the GameStop Stock Price Dynamics and Trading Volume

A co-integration analysis is used to test the relationship between the mean-reverting force in the GME price dynamics and the daily trading volume using Equation (7), where y_t is κ or θ at time t , and X_{t-1} is the logarithm of the trading volume at time $t-1$. The estimation is conducted at a daily frequency from 1 January 2019 to 21 January 2021. Table 5 reports the summary statistics, correlation coefficient, and respective ADF test results for the variables both in levels and first differences, suggesting that these three variables are co-integrated in the same order I(1) at a 1% significance level.

Table 5. Descriptive statistics of $\ln(\text{volume})$, κ , and θ of GameStop stock price.

	κ		θ		$\ln(\text{volume})$				
	Level	Change	Level	Change	Level	Change			
Mean	0.04	0.000	0.91	-0.002	15.37	0.006			
Median	0.04	0.000	0.94	0.002	15.26	-0.031			
Maximum	0.08	0.017	1.47	0.428	18.79	3.140			
Minimum	0.00	-0.024	0.01	-0.426	14.06	-1.676			
Std. Dev.	0.02	0.002	0.25	0.064	0.73	0.561			
Skewness	0.87	-1.118	-0.65	-0.271	1.25	1.043			
Kurtosis	2.81	44.585	3.42	13.705	5.41	7.352			
ADF test statistics	-0.64	-27.62	***	-1.94	-22.938	***	0.32	-16.79	***
Phillips-Perron test statistics	-0.63	-27.86	***	-2.01	-22.944	***	-9.76	-67.73	***
Correlation with $\ln(\text{vix})$	-0.34	-	-0.44	-	-	-	-	-	-
Observations	518	517	518	517	518	517			

Notes: *** indicates significance at a level of 1%. Both tests check the null hypothesis of unit root existence in the time series.

Table 6 reports the co-integration tests between $\ln(\text{volume})$ and (κ, θ) , showing the presence of at least one co-integrating vector between $\ln(\text{volume})$ and (κ, θ) , respectively, at 5% or 1% significance levels. The co-integrating vectors between $\ln(\text{volume})$ and (κ, θ) expressed by β , as shown in Table 7, are estimated to be -0.003 and -0.15 at the 1% significance level, respectively. The estimated negative coefficients indicate that a higher trading volume reduces κ and θ , suggesting that the restoring force in the GME price dynamics weakens with a higher trading volume. Table 8 illustrates that the speeds of adjustment (α_y) for κ and θ are negative, showing that the gap between the model parameters and the trading volume will be closed subsequently.

Table 6. Tests for co-integration of $\ln(\text{volume})$, κ , and θ of GameStop stock price.

Engle-Granger Single-Equation Test	κ		θ	
Dependent Variable:				
ADF test statistic	-2.51	**	-3.69	***
Phillips-Perron test statistic	-3.84	**	-4.00	***

Notes: *** and ** indicate significance at levels of 1% and 5%, respectively. The cointegration test uses the Augmented Dickey-Fuller and Phillips-Perron tests to check the null hypothesis that the residuals of the regression of $\ln(\text{volume})$ and the parameters from the MLE calibration with a 2-year rolling window are non-stationary. The critical value of the test was obtained from MacKinnon (1996).

Table 7. Estimates of long-run coefficient (β) for $\ln(\text{volume})$, κ , and θ of GameStop stock price.

Dependent Variable:	κ		θ	
$\ln(\text{volume})$	-0.003	***	-0.15	***
Constant	0.094	***	3.23	***

Note: 1. *** indicates significance at a level of 1%.

Table 8. Estimation results of the short-run dynamics for $\ln(\text{volume})$, κ , and θ of GameStop stock price.

Dependent Variable:	κ		θ	
$\ln(\text{volume})$				
Speed of adjustment	−0.011	**	−0.03	**
Lag length	1		1	

Note: ** indicates significance at a level of 5%.

5. Conclusions

A simple stochastic approach has been presented for modelling equity prices under shocks which are constrained to lie within a band. The model is able to capture most stylised facts of equity prices. While the proposed stochastic process has a quasi-bounded boundary which can be breached if the probability leakage condition is met, the other boundary of the band is an inaccessible boundary. The quasi-boundedness at the boundary can be considered a measure of possible downside or upside risk of the corresponding equity prices.

The empirical results show that the S&P500 dynamics can be calibrated according to the quasi-bounded process, in which the volatility and mean-reversion are positively and negatively co-integrated, respectively, with the VIX index, representing the market distress risk implied in the option market. The process also captures the default risk incorporated in stock prices. Hertz filed for Chapter 11 bankruptcy in May 2020 as a result of the COVID-19 pandemic. The volatility and mean-reversion of the calibrated Hertz stock price dynamics are positively and negatively related, respectively, to the number of COVID-19 cases. The process indicates a high likelihood of default in terms of the probability leakage condition at the lower boundary in March 2020 using only information until that point.

The proposed stochastic approach is also able to model equity price dynamics under a short squeeze. A quasi-bounded moving upper bound is the threshold imposed by constraints, such as stop-loss limits forcing traders to close out their short-selling positions squeezed by co-ordinated long-buying. Calibration of the process for the GameStop stock price shows that the quasi-bounded property can adequately describe the price dynamics. The model captures the short squeeze of the stock, as indicated by its price dynamics, when the probability leakage condition for breaching the upper bound was met on 14 January 2021 using only information until that point, i.e., about two weeks before major short-sellers closed out their positions with a significant loss. The trading volume of the stock is negatively co-integrated with the mean reversion of the dynamics, suggesting overshooting prices with increased trading volume during co-ordinated short squeezes.

Given the availability of an analytically tractable probability density function, empirical calibration of the model parameters of the proposed process for different financial observables in general can also be easily performed. Hence, making predictions of future movements of these observables becomes feasible. The leakage condition at the quasi-bounded boundary can thus provide us with a forward-looking indicator of potential crash risk or short squeeze of the corresponding financial observables, including equities for risk management purposes. While only a limited number of firms' equity prices are calibrated in this sample, we leave the investigation of a larger sample of companies in distress or experiencing short squeeze for future research. In addition, one of the limitations of this study is that fundamental factors such as a firm's balance-sheet information is not incorporated into the model. Future theoretical research on equity price dynamics could incorporate such factors.

Author Contributions: C.-H.H. and C.-F.L. are responsible for proposing the model and deriving the corresponding stochastic processes. C.-H.L. is responsible for performing the calibration of model parameters. All authors have read and agreed to the published version of the manuscript.

Funding: This research received no external funding.

Data Availability Statement: The datasets used in this paper are available from Bloomberg and the Johns Hopkins University Center for Systems Science and Engineering (JHU CCSE) at <https://data.humdata.org/dataset/novel-coronavirus-2019-ncov-cases> (accessed on 15 September 2020).

Acknowledgments: The views expressed in this paper are the authors' and do not represent those of the Hong Kong Monetary Authority.

Conflicts of Interest: The authors declare no conflicts of interest.

References

- Asness, Clifford S., Tobias J. Moskowitz, and Lasse Heje Pedersen. 2013. Value and momentum everywhere. *Journal of Finance* 68: 929–85. [CrossRef]
- Bates, David S. 2012. U.S. stock market crash risk, 1926–2010. *Journal of Financial Economics* 105: 229–59. [CrossRef]
- Black, Fischer. 1986. Noise. *Journal of Finance* 41: 529–43. [CrossRef]
- Boehmer, Ekkehart, Charles M. Jones, and Xiaoyan Zhang. 2008. Which shorts are informed? *Journal of Finance* 63: 491–527. [CrossRef]
- Boualam, Yasser, João F. Gomesz, and Colin Wardx. 2020. *Understanding the Behavior of Distressed Stocks*. Working Paper. Chapel Hill: University of North Carolina.
- Bouchaud, Jean-Philippe, Philipp Krueger, Augustin Landier, and David Thesmar. 2019. Sticky expectations and the profitability anomaly. *Journal of Finance* 74: 639–74. [CrossRef]
- Bouchaud, Jean-Philippe, Stefano Ciliberti, Yves Lempérière, Adam Aleksander Majewski, Philip Seager, and Kévin Sin Ronia. 2018. Black Was Right: Price Is within a Factor 2 of Value. *risk.net*, October 10. Available online: <https://www.risk.net/cutting-edge/investments/6004766/black-was-right-price-is-within-a-factor-2-of-value> (accessed on 1 December 2023).
- Brunnermeier, Markus K., and Lasse Heje Pedersen. 2005. Predatory trading. *Journal of Finance* 60: 1825–63. [CrossRef]
- Brunnermeier, Markus K., and Martin Oehmke. 2014. Predatory short selling. *Review of Finance* 18: 2153–95. [CrossRef]
- Brunnermeier, Markus K., Stefan Nagel, and Lasse Heje Pedersen. 2009. Carry trades and currency crashes. *NBER Macroeconomics Annual* 23: 313–47. [CrossRef]
- Cardeal, João Azevedo, Marc de Montigny, F. C. Khanna, Tarcisio M. Rocha Filho, and A. E. Santana. 2007. Galilei-invariant gauge symmetries in Fokker-Planck dynamics with logarithmic diffusion and drift terms. *Journal of Physics A: Mathematical and Theoretical* 40: 13467. [CrossRef]
- Carr, Peter, Andrey Itkin, and Dmitry Muravey. 2020. Semi-closed form prices of barrier options in the time-dependent CEV and CIR models. *Journal of Derivatives* 28: 26–50. [CrossRef]
- Conrad, Jennifer, Nishad Kapadia, and Yuhang Xing. 2014. Death and jackpot: Why do individual investors hold overpriced stocks? *Journal of Financial Economics* 113: 455–75. [CrossRef]
- Cox, J. C., J. E. Ingersoll, and S. A. Ross. 1985. A theory of the term structure of interest rates. *Econometrica* 53: 385–407. [CrossRef]
- Daniel, Kent, David Hirshleifer, and Avanidhar Subrahmanyam. 1998. Investor psychology and security market under- and over-reactions. *Journal of Finance* 53: 1839–85. [CrossRef]
- Day, Richard H., and Weihong Huang. 1990. Bulls, bears and market sheep. *Journal of Economic Behavior and Organization* 14: 299–329. [CrossRef]
- de Bondt, Werner, and Richard H. Thaler. 1985. Does the stock market overreact? *Journal of Finance* 42: 557–81. [CrossRef]
- DeLong, J. Bradford, Andrei Shleifer, Lawrence H. Summers, and Robert J. Waldmann. 1990. Positive feedback investment strategies and destabilizing rational speculation. *Journal of Finance* 45: 379–95. [CrossRef]
- Diether, Karl B., Kuan-Hui Lee, and Ingrid M. Werner. 2009. Short sale strategies and return predictability. *Review of Financial Studies* 22: 575–607. [CrossRef]
- Eisdorfer, Assaf, Amit Goyal, and Alexei Zhdanov. 2019. Equity misvaluation and default options. *Journal of Finance* 74: 845–98. [CrossRef]
- Elkamhi, Redouane, Jan Ericsson, and Christopher A. Parsons. 2012. The cost of financial distress and the timing of default. *Journal of Financial Economics* 105: 62–81. [CrossRef]
- Engle, Robert F., and Clive W.J. Granger. 1987. Co-integration and error correction: Representation, estimation and testing. *Econometrica* 55: 251–76. [CrossRef]
- Fama, Eugene F., and Kenneth R. French. 1988. Permanent and temporary components of stock prices. *Journal of Political Economy* 96: 246–73. [CrossRef]
- Gao, Pengjie, Christopher A. Parsons, and Jianfeng Shen. 2017. Global relation between financial distress and equity returns. *Review of Financial Studies* 31: 239–77. [CrossRef]
- Hackbarth, Dirk, Rainer Haselmann, and David Schoenherr. 2015. Financial distress, stock returns, and the 1978 bankruptcy reform act. *Review of Financial Studies* 28: 1810–47. [CrossRef]
- Heston, Steven L. 1993. A closed-form solution for options with stochastic volatility with applications to bond and currency options. *Review of Financial Studies* 6: 327. [CrossRef]
- Hong, Harrison, and Jeremy Stein. 1999. A unified theory of underreaction, momentum trading, and overreaction in asset markets. *Journal of Finance* 54: 2143–84. [CrossRef]

- Hui, Cho-Hoi, Andrew Wong, and Chi-Fai Lo. 2022. A note on modelling yield curve control: A target-zone approach. *Finance Research Letters* 49: 103076. [\[CrossRef\]](#)
- Hui, Cho-Hoi, Chi-Fai Lo, and Tom Fong. 2016. Swiss franc's one-sided target zone during 2011–2015. *International Review of Economics and Finance* 44: 54–67. [\[CrossRef\]](#)
- Ingersoll, Jonathan E., Jr. 1997. Valuing foreign exchange rate derivatives with a bounded exchange process. *Review of Derivatives Research* 1: 159–81. [\[CrossRef\]](#)
- Jurek, Jakub W. 2014. Crash-neutral currency carry trades. *Journal of Financial Economics* 113: 325–47. [\[CrossRef\]](#)
- Karlin, Samuel, and Howard M. Taylor. 1981. *A Second Course in Stochastic Processes*. New York: Academic Press.
- Larsen, Kristian Stegenborg, and Michael Sørensen. 2007. A diffusion model for exchange rates in a target zone. *Mathematical Finance* 17: 285–306. [\[CrossRef\]](#)
- Lempérière, Yves, Cyril Deremble, Philip Seager, Marc Potters, and Jean-Philippe Bouchaud. 2014. Two centuries of trend following. *Journal of Investment Strategies* 3: 41–61. [\[CrossRef\]](#)
- Lo, Chi-Fai, Cho-Hoi Hui, Tom Fong, and S. W. Chu. 2015. A quasi-bounded target zone model—Theory and application to Hong Kong dollar. *International Review of Economics and Finance* 37: 1–17. [\[CrossRef\]](#)
- Lux, Thomas, and Michele Marchesi. 2000. Volatility clustering in financial markets: A microsimulation of interacting agents. *International Journal of Theoretical and Applied Finance* 3: 675–702. [\[CrossRef\]](#)
- MacKinnon, James G. 1996. Numerical distribution functions for unit root and cointegration test. *Journal of Applied Econometrics* 11: 601–18. [\[CrossRef\]](#)
- Madan, Dilip B. 2017. Pricing options on mean reverting underliers. *Quantitative Finance* 17: 497–513. [\[CrossRef\]](#)
- McQuade, Timothy. 2018. *Stochastic Volatility and Asset Pricing Puzzles*. Working Paper. Berkeley: University of California.
- Nartea, Gilbert V., Harold Glenn A. Valera, and Maria Luisa G. Valera. 2021. Mean reversion in Asia-Pacific stock prices: New evidence from quantile unit root tests. *International Review of Economics & Finance* 73: 214–30.
- Opp, Christian C. 2021. *Large Shareholders and Financial Distress*. Working Paper. Rochester: University of Rochester.
- Pesz, Karol. 2002. A class of Fokker-Planck equations with logarithmic factors in diffusion and drift terms. *Journal of Physics A: Mathematical and General* 35: 1827–32. [\[CrossRef\]](#)
- Ritschel, Stefan, Andrey G. Cherstvy, and Ralf Metzler. 2021. Universality of delay-time averages for financial time series: Analytical results, computer simulations, and analysis of historical stock-market prices. *Journal of Physics: Complex* 2: 045003. [\[CrossRef\]](#)
- Silva, Erica M., Tarcisio M. Rocha Filho, and Ademir E. Santana. 2006. Lie symmetries of Fokker-Planck equations with logarithmic diffusion and drift terms. *Journal of Physics: Conference Series* 40: 150–55. [\[CrossRef\]](#)
- Stein, Jeremy. 2009. Sophisticated investors and market efficiency. *Journal of Finance* 64: 1517–48. [\[CrossRef\]](#)
- Vinod, Deepak, Andrey G. Cherstvy, Ralf Metzler, and Igor M. Sokolov. 2022. Time-averaging and nonergodicity of reset geometric Brownian motion with drift. *Physical Review E* 106: 034137. [\[CrossRef\]](#) [\[PubMed\]](#)

Disclaimer/Publisher's Note: The statements, opinions and data contained in all publications are solely those of the individual author(s) and contributor(s) and not of MDPI and/or the editor(s). MDPI and/or the editor(s) disclaim responsibility for any injury to people or property resulting from any ideas, methods, instructions or products referred to in the content.